arXiv:1607.05082v1 [hep-lat] 18 Jul 2016

# Finite Temperature Lattice QCD - Baryons in the Quark-Gluon Plasma

Gert Aarts, Chris Allton, Davide De Boni, Simon Hands, Benjamin Jäger[†], Chrisanthi Praki,

Department of Physics, College of Science, Swansea University, Swansea SA2 8PP, United Kingdom

Jon-Ivar Skullerud

Department of Mathematical Physics, National University of Ireland Maynooth, Maynooth, County Kildare, Ireland
School of Mathematics, Trinity College, Dublin 2, Ireland

Baryonic correlation functions provide an ideal tool to study parity doubling and chiral symmetry using lattice simulations. We present a study using $2 + 1$ flavors of anisotropic Wilson clover fermions on the FASTSUM ensembles and find clear evidence that parity doubling emerges in the quark-gluon plasma. This result is confirmed on the level of spectral functions, which are obtained using a MEM reconstruction. We further highlight the importance of Gaussian smearing in this study.

PACS numbers: 12.38.Gc, 12.38.-t, 12.38.Mh, 12.38.Aw

## 1. Introduction

Symmetries are essential to understand interactions in nature and have led to many discoveries in the past. Here we study baryons at nonzero temperature, for which, in contrast to mesons, not many lattice studies are available [1–4]. We focus in particular on parity doubling and chiral symmetry restoration, which are expected to coincide for a phase where chiral symmetry is manifest. In a previous study [5, 6], we focused on correlation function itself; here we extend our study to include spectral functions and different levels of smearing.

[†] Presented at the Workshop "Excited QCD 2016", Portugal, 6-12 March 2016.

## 2. Setup

We use non-perturbatively $\mathcal{O}(a)$ improved, anisotropic Wilson fermions with $2+1$ flavors on configurations generated by the FASTSUM collaboration [7–9], based on the parameters of the Hadron Spectrum Collaboration [10]. The simulation parameter are listed in table 1. These ensembles

| $N_s$ | $N_t$ | $T$[MeV] | $T/T_c$ | $N_{\text{cfg}}$ | $N_{\text{src}}$ |
|---|---|---|---|---|---|
| 24 | 128 | 44 | 0.24 | 171 | 2 |
| 24 | 40 | 141 | 0.76 | 301 | 4 |
| 24 | 36 | 156 | 0.84 | 252 | 4 |
| 24 | 32 | 176 | 0.95 | 1000 | 2 |
| 24 | 28 | 201 | 1.09 | 501 | 4 |
| 24 | 24 | 235 | 1.27 | 1001 | 2 |
| 24 | 20 | 281 | 1.52 | 1000 | 2 |
| 24 | 16 | 352 | 1.90 | 1001 | 2 |

Table 1. Simulation parameters.

span a wide range in temperatures, ranging from 44 MeV to 352 MeV, and in terms of the critical temperature from 0.24 to $1.9\,T_c$. We use a fixed spatial lattice spacing of $a_s = 0.1227(8)$ fm and a finer lattice spacing in the time directions, such that the anisotropy is $a_s/a_t = 3.5$ [11]. The strange quark mass has been tuned to its physical value, while the light quarks remain heavier than in nature, which results in a pion mass of 384(4) MeV [11]. Further details of the ensembles can be found in [7–9].

For the nucleon interpolating operator we use a standard definition (see e.g. [12, 13]),

$$O_N = \epsilon_{abc}\, u_a \,(u_b\, C\gamma_5\, d_c)\,. \tag{1}$$

With this definition and the projector to positive parity $P_+ = \frac{1}{2}\,(\mathbb{1} + \gamma_4)$, the correlation function of the nucleon can be obtained by

$$C(t) = \sum_{\vec{x}} \langle O_N(\vec{x}, t)\, P_+\, \overline{O_N}(0)\rangle. \tag{2}$$

To enhance the overlap with the ground state, we employ Gaussian smearing [14] on the source and the sink operator of the correlation functions, which will be discussed below. It will become clear that smearing is crucial for separating out the ground state already at early Euclidean times. Since Wilson fermions explicitly break chiral symmetry, we do not expect that all excited states reflect parity doubling and hence we focus in this work on the low-energy states. The correlation functions have been computed using the Chroma software package [15].

## 3. Results

The left panel of figure 1 shows the correlation functions for various temperatures. The individual correlation function is the result of super-

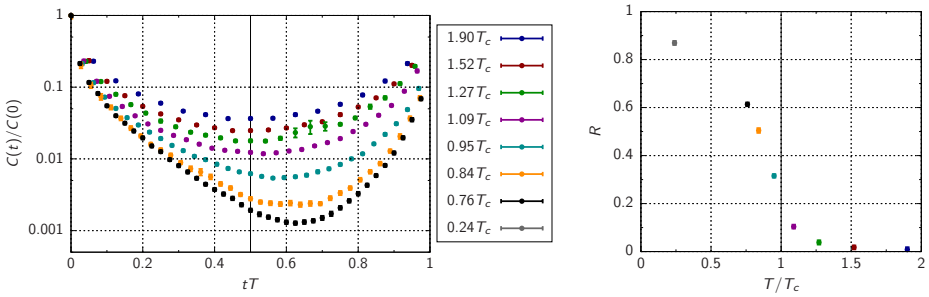


Figure 1. Left: Correlation functions of the nucleon for different temperatures, as a function of $tT$. Right: The weighted average $R$, defined in equation 3, as a function of temperature. The error bars in both panels are of the order of the symbol size.

position of forward-propagating states with positive parity and backward-propagating states with negative parity. In nature, the ground states in each channel have different masses resulting in asymmetric correlation functions. This behaviour is clearly reproduced in figure 1 for $T < T_c$. As the temperature the correlation function regains more and more of its reflection symmetry around $tT = 1/2$, which indicates the emergence of parity doubling in the quark-gluon plasma. To quantify this further, we look at a weighted average of ratios of correlation functions [3],

$$R = \frac{1}{Z} \sum_{i=1}^{N_t/2-1} R(t_i)/\sigma_i^2, \quad \text{where} \quad R(t) = \frac{C(t) - C(N_t - t)}{C(t) + C(N_t - t)} \tag{3}$$

and $Z = \sum_i \sigma_i^{-2}$ is the normalization. The right panel of figure 1 shows this ratio $R$, which shows a crossover behaviour and confirms the coincidence of parity doubling with the thermal transition.

Looking at the spectral decomposition of the correlations functions,

$$C(t) = \int_{-\infty}^{\infty} \frac{\mathrm{d}\omega}{2\pi} K(t,\omega)\, \rho(\omega), \tag{4}$$

allows us to study properties of the nucleon system further. The determination of the spectral function $\rho(\omega)$ is an ill-posed problem in itself, which we study by using the Maximum Entropy Method (MEM) [16] and adapting the kernel $K(t,\omega)$ to this (fermionic) problem. For the correlator shown in

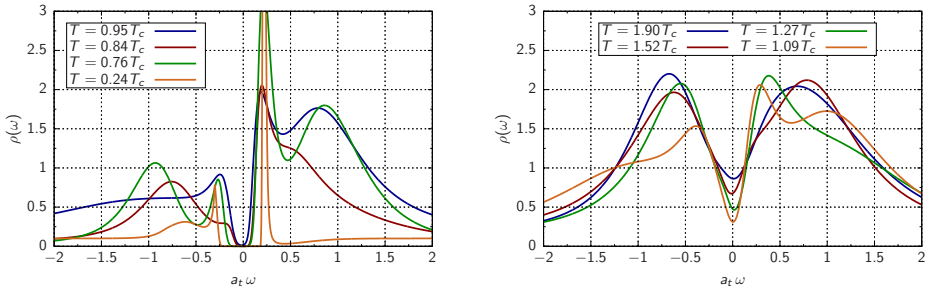


Figure 2. The spectral function of the nucleon for a variety of temperatures below the critical temperature (left) and above the critical temperature (right).

figure 1, the kernel reads [17]

$$K(t,\omega) = \frac{\mathrm{e}^{-\omega t}}{1+\mathrm{e}^{-\omega/T}}. \tag{5}$$

Figure 2 shows the result of this spectral reconstruction. Note that the spectrum at positive (negative) $\omega$ corresponds to the positive (negative) parity channel. At low temperatures the ground states in both the positive and negative parity channels are clearly visible, but they are reduced as the temperature increases. Above $T_c$ the spectral function becomes more and more symmetric, consistent with the analysis from the correlators directly.

As mentioned before, we apply Gaussian smearing [14] to the source and the sink operator, i.e.

$$\psi'(x) = \frac{1}{A}\left(\mathbb{1} + \kappa\, H\right)^n \psi(x), \tag{6}$$

where $H$ corresponds to the hopping part of the Dirac operator and $A$ is an appropriate normalization. The links variables in $H$ are APE smeared [18]. In total, we apply four different settings for the smearing parameters $\kappa$ and $n$,

$$(\kappa, n) = (0,0);\ (1.2,10);\ (4.2,60);\ (8.7,140), \tag{7}$$

to test the dependence on the smearing, which includes a setup with no smearing at all. The data shown in the first part of this section, i.e. figures 1 and 2, have been obtained using $(\kappa = 8.7, n = 140)$. The left panel of figure 3 shows the resulting spectral functions for an ensemble with a temporal extent of $N_t = 40$. As expected the overlap with the ground state changes significantly by changing the spectral weights with the smearing procedure. The position of the first peak, i.e the mass of the ground state, remains however unchanged. As far as our analysis and uncertainties allow,

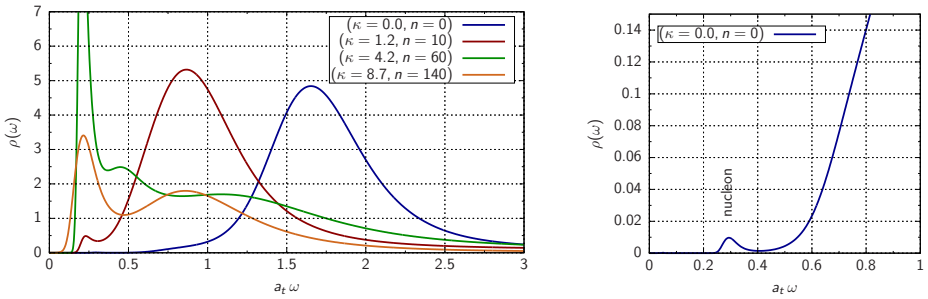


Figure 3. The effect of smearing on one particular ensemble with $N_\tau = 40$, showing only the positive parity sector. Left: A comparison of various levels of smearing as listed in equation (7). Right: A zoom of the spectral function without smearing.

we also see no clear change in the width, which still needs more data to be confirmed. In particular without any smearing the ground state is severely suppressed, but still visible, and this is clearly shown in the right panel of figure 3. Therefore smearing is absolutely crucial for extracting information on the ground state.

## 4. Conclusion

We have presented a lattice study of the spin-$\frac{1}{2}$ octet nucleon in the hadronic phase and quark-gluon plasma, spanning a wide range of temperatures across the transition. We find clear evidence of parity doubling and thereby chiral symmetry restoration in the quark-gluon plasma, which is further confirmed on the level of the spectral functions. Gaussian smearing has shown to be essential in this work. In future we will extend our study to the spin-$\frac{3}{2}$ baryon decuplet and include different valence quark masses.

## 5. Acknowledgements

We are grateful for the computing resources made available by HPC Wales. We acknowledge the STFC grants ST/L000369/1, ST/K000411/1, ST/H008845/1, ST/K005804/1 and ST/K005790/1, the STFC DiRAC HPC Facility (www.dirac.ac.uk), PRACE grants 2011040469 and Pra05 1129q, CINECA grant INF14 FTeCP (CINECA-INFN agreement). We thank the Royal Society, the Wolfson Foundation and the Leverhulme Trust for their support.

References

[1] C. E. DeTar and J. B. Kogut, Phys. Rev. Lett. **59** (1987) 399.

[2] C. E. DeTar and J. B. Kogut, Phys. Rev. D **36** (1987) 2828.

[3] S. Datta, S. Gupta, M. Padmanath, J. Maiti and N. Mathur, JHEP **1302** (2013) 145 doi:10.1007/JHEP02(2013)145 [arXiv:1212.2927 [hep-lat]].

[4] I. Pushkina *et al.* [QCD-TARO Collaboration], Phys. Lett. B **609** (2005) 265 [hep-lat/0410017].

[5] G. Aarts, C. Allton, S. Hands, B. Jäger, C. Praki and J. I. Skullerud, Phys. Rev. D **92** (2015) no.1, 014503 doi:10.1103/PhysRevD.92.014503 [arXiv:1502.03603 [hep-lat]].

[6] G. Aarts, C. Allton, S. Hands, B. Jäger, C. Praki and J. I. Skullerud, PoS LATTICE **2015** (2015) 183 [arXiv:1510.04040 [hep-lat]].

[7] A. Amato, G. Aarts, C. Allton, P. Giudice, S. Hands and J. I. Skullerud, Phys. Rev. Lett. **111** (2013) 172001 [arXiv:1307.6763 [hep-lat]].

[8] G. Aarts, C. Allton, A. Amato, P. Giudice, S. Hands and J. I. Skullerud, JHEP **1502** (2015) 186 [arXiv:1412.6411 [hep-lat]].

[9] G. Aarts, C. Allton, T. Harris, S. Kim, M. P. Lombardo, S. M. Ryan and J. I. Skullerud, JHEP **1407** (2014) 097 doi:10.1007/JHEP07(2014)097 [arXiv:1402.6210 [hep-lat]].

[10] R. G. Edwards, B. Joo and H. W. Lin, Phys. Rev. D **78** (2008) 054501 [arXiv:0803.3960 [hep-lat]].

[11] H. W. Lin *et al.* [Hadron Spectrum Collaboration], Phys. Rev. D **79** (2009) 034502 [arXiv:0810.3588 [hep-lat]].

[12] I. Montvay and G. Münster, "Quantum fields on a lattice," Cambridge, UK: Univ. Pr. (1994) 491 p. (Cambridge monographs on mathematical physics).

[13] C. Gattringer and C. B. Lang, "Quantum chromodynamics on the lattice," Lect. Notes Phys. **788** (2010) 1.

[14] S. Güsken, U. Low, K. H. Mütter, R. Sommer, A. Patel and K. Schilling, Phys. Lett. B **227** (1989) 266.

[15] R. G. Edwards *et al.* [SciDAC and LHPC and UKQCD Collaborations], Nucl. Phys. Proc. Suppl. **140** (2005) 832 [hep-lat/0409003].

[16] M. Asakawa, T. Hatsuda and Y. Nakahara, Prog. Part. Nucl. Phys. **46** (2001) 459 [hep-lat/0011040].

[17] C. Praki and G. Aarts, PoS LATTICE **2015** (2015) 182 [arXiv:1510.04069 [hep-lat]].

[18] M. Albanese *et al.* [APE Collaboration], Phys. Lett. B **192** (1987) 163.